Aust. J. Phys., 1989, **42**, 101–11

Observation of Spatial Variations in the Energy Distribution Function for Steady-state Townsend Discharges

A. B. Wedding[A] *and L. J. Kelly*

School of Physical Sciences, Flinders University of South Australia,
Bedford Park, S.A. 5042, Australia.
[A] Present address: Department of Physics,
University of Western Australia, Nedlands, W.A. 6009, Australia.

Abstract

Spatial variations of the relative excitation rates for two electronic states of molecular nitrogen have been measured for a point source Townsend discharge. The ratio of these rates shows a spatial dependence which is explained in terms of an electron concentration gradient expansion of the energy distribution function. The electronic states were chosen to have quite different threshold energies such that the ratio would be sensitive to small changes in the electron energy distribution. A model for secondary electron production is used to explain the significant influence of secondary electrons in the outer regions of the discharge.

1. Introduction

In a Townsend discharge the electron energy distribution is a function of E/N (E is the electric field strength and N is the concentration of neutral gas molecules) and the local gradient of the electron concentration (Thomas 1969; Kumar *et al.* 1980). One of the more obvious consequences of this dependence on concentration gradients is the difference between the longitudinal and transverse diffusion coefficients D_L and D_T (Parker and Lowke 1969; Skullerud 1969). In the presence of ionisation or attachment there are also consequent changes to both the diffusion tensor and the electron drift velocity W (Tagashira *et al.* 1977; Blevin and Fletcher 1984). However, these changes in the transport coefficients are an indirect indication of spatial changes in the energy distribution function and a heavy reliance on theory is required to make this connection.

The present work describes measurements of the relative excitation rates for two electronic states of nitrogen, namely the 337·1 nm (0,0) band of the second positive system and the 391·4 nm (0,0) band of the first negative system. The ratio of these rates in a steady-state Townsend discharge would be expected to exhibit a spatial dependence resulting from spatial gradients of the electron concentration. This method of investigation gives a direct indication of spatial variations in the electron energy distribution function.

2. Theoretical Model for a Steady-state Townsend Discharge

When a group of electrons leaves the cathode they attain an equilibrium energy distribution only after being displaced a distance of the order a few

0004-9506/89/010101$03.00

times D_T/W (Robson 1981; Blevin 1985). We define the quantities $\lambda_L = W/2D_L$ and $\lambda_T = W/2D_T$ so that $\lambda_L z$ and $\lambda_T r$ are dimensionless variables in the axial and radial directions of the cylindrical discharge, with the electric field in the negative z direction. The problem of calculating the electron concentration in a steady-state discharge when the influence of boundaries and initial conditions is included has not been solved using analytic methods (Kumar *et al.* 1980; Robson 1981). For the purposes of this paper a determination of the electron concentration $n(r, z)$ and concentration gradients is carried out using a dipole source at the cathode ($r = 0, z = 0$), together with an image term to satisfy the assumed boundary condition that $n = 0$ at the anode, $z = d$. No allowance is made for the detailed structure of the boundary layer regions near the electrodes.

Following Huxley (1972), and including the anode image term, the electron concentration is given by

$$n(r, z) = \text{const.}\, \lambda_L z \exp(\lambda_L z)\left(\frac{K_{3/2}(S_1)}{S_1^{3/2}} - \frac{2d - z}{z}\,\frac{K_{3/2}(S_2)}{S_2^{3/2}}\right), \tag{1}$$

where

$$S_1(r, z) = \lambda_L z\left(1 - \frac{2\nu_i^0}{W\lambda_L}\right)^{\frac{1}{2}}\left\{1 + \frac{\lambda_L}{\lambda_T}\left(\frac{\lambda_T r}{\lambda_L z}\right)^2\right\}^{\frac{1}{2}},$$

$$S_2(r, z) = S_1(r, 2d - z),$$

and $K_{3/2}(S)$ is a modified Bessel function of the second kind. The ionisation frequency ν_i^0 is the value corresponding to a region of constant electron concentration, or equivalently, the value averaged over an isolated swarm (Blevin and Fletcher 1984). Equation (1) may be expected to give semi-quantitative results provided that $\lambda_L z \geq 1$ and the discharge is observed in regions remote from the anode. The applicability of this description to photon emission experiments of the type described in this work has been demonstrated (Wedding *et al.* 1985, and references therein).

For cylindrical symmetry the energy distribution function $f(r,z,\epsilon)$ can be expressed in an electron concentration gradient expansion as

$$f(r,z,\epsilon) = n(r,z)\,g^0(\epsilon) - \frac{1}{\lambda_L}\,\frac{\partial n(r,z)}{\partial z}\,g^1(\epsilon) + \ldots,$$

where only the first two terms will be retained since numerical calculations indicate that these are the dominant terms (Tagashira *et al.* 1977). The expansion differs from that used by Blevin and Fletcher (1984), since λ_L is used instead of N in the second term to render $g^1(\epsilon)$ independent of pressure. This change also ensures that $g^0(\epsilon)$ and $g^1(\epsilon)$ have the same dimensions. The normalised energy distribution function is then

$$\frac{f(r,z,\epsilon)}{n(r,z)} = g^0(\epsilon) - 2\left(D_L\,\frac{\partial n(r,z)}{\partial z}\Big/ Wn(r,z)\right)g^1(\epsilon), \tag{2}$$

so that the coefficient of $g^1(\epsilon)$ is twice the ratio of the axial diffusion flux to the drift flux. If the absolute value of this coefficient is of order unity, it would be expected that the local rate of energy gain from the field would be significantly different to the situation where there are no concentration gradients. Consequently, $(1/\lambda_L n)\partial n/\partial z$ calculated from equation (1) gives an indication of those regions in the discharge where large variations in the excitation rate may occur.

Note that the normalised energy distribution function for a one-dimensional Townsend discharge, with $n(z) = \text{const.}\exp(\alpha_T z)$, is

$$\frac{f(z,\epsilon)}{n(z)} = g^0(\epsilon) - \frac{\alpha_T}{\lambda_L} g^1(\epsilon). \tag{3}$$

The spatially dependent excitation frequency to a state j with excitation cross section $Q_j(\epsilon)$ is then

$$\nu_{\text{ex}j}(r,z) = \nu^0_{\text{ex}j} - \left(\frac{1}{\lambda_L n(r,z)} \frac{\partial n(r,z)}{\partial z}\right) \nu^1_{\text{ex}j}, \tag{4}$$

where

$$\nu^0_{\text{ex}j} = N\left(\frac{2}{m}\right)^{\frac{1}{2}} \int_0^\infty \epsilon^{\frac{1}{2}} Q_j(\epsilon)\, g^0(\epsilon)\, \mathrm{d}\epsilon$$

corresponds to the excitation frequency in the absence of spatial gradients (or the spatially averaged value for an isolated swarm), and

$$\nu^1_{\text{ex}j} = N\left(\frac{2}{m}\right)^{\frac{1}{2}} \int_0^\infty \epsilon^{\frac{1}{2}} Q_j(\epsilon)\, g^1(\epsilon)\, \mathrm{d}\epsilon.$$

It follows from equation (4) that $\nu_{\text{ex}j}(r,z) > \nu^0_{\text{ex}j}$ when $\partial n/\partial z$ is negative and the axial diffusion flux adds to the drift flux. Conversely, $\nu_{\text{ex}j}(r,z) < \nu^0_{\text{ex}j}$ when $\partial n/\partial z$ is positive. To illustrate the spatial variations which may be expected under typical experimental conditions, equation (1) has been used to plot contours of equal electron concentration as shown in Fig. 1. In this example experimentally determined transport coefficients for a $CO_2 : N_2 : He : CO$ mixture (Wedding 1985) at 300 Td (1 Td $\equiv 10^{-17}$ V cm^2) were used, i.e. $\lambda_L/\lambda_T = 1 \cdot 095$ and $2\nu^0_i/W\lambda_L = 0 \cdot 185$. These results are approximate in that the anode and cathode boundary conditions are not exactly accounted for. However, it is clear that for small values of z large negative axial gradients are found near the axis, but change sign as r increases. For larger values of z the gradients are positive for all values of r.

The corresponding values of $(1/\lambda_L n)\partial n/\partial z$ as a function of radial position are shown in Fig. 2 for several axial positions. Only at large values of z does $(1/\lambda_L n)\partial n/\partial z$ approach α_T/λ_L, the value expected for a one-dimensional Townsend discharge from equation (3).

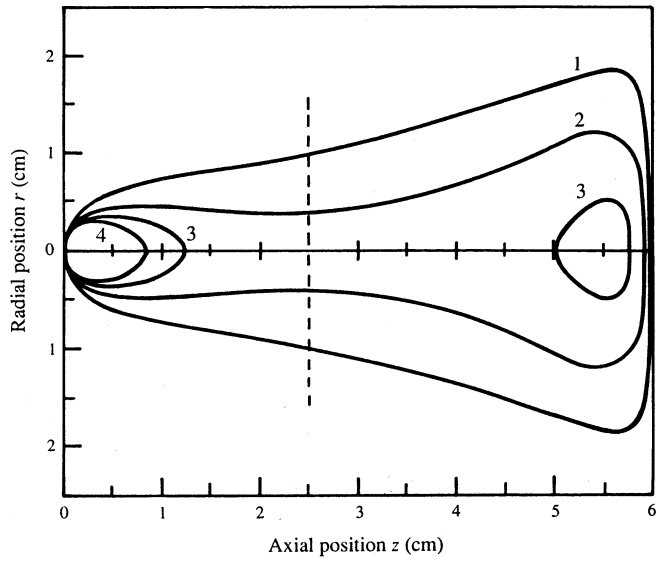

Fig. 1. Contours of constant electron concentration within a steady stream discharge for the following conditions: $E/N = 300$ Td, $p_0 = 0 \cdot 37$ Torr, $W = 45$ cm μs^{-1}, $\alpha_T/p_0 = 1 \cdot 0$ cm^{-1} Torr^{-1}, $D_T/\mu = 5 \cdot 20$ V and $D_L/\mu = 4 \cdot 75$ V. (The concentration is given in arbitrary units.)

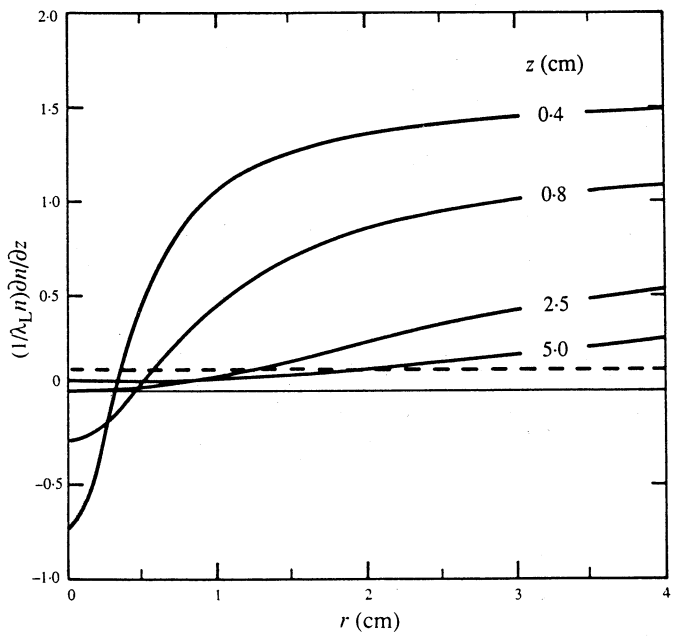

Fig. 2. Radial variation of $(1/\lambda_L n)\partial n/\partial z$ for several axial positions. The spatially independent limit which is approached for large z is given by equation (3) as α_T/λ_L (dashed line).

3. Experimental Results

The apparatus used in these experiments has been described in detail elsewhere (Wedding *et al.* 1985), so that only a brief description of the procedures will be given here. A Townsend discharge was established between two parallel plate electrodes with a separation of 6·0 cm. Guard rings of internal radius $R = 5 \cdot 5$ cm were spaced every 1·0 cm to maintain a uniform electric field. Discharges were studied in pure molecular nitrogen, a N_2 and He mixture (N_2 : He = 75 : 25) and a $CO_2 : N_2 : He : CO$ (6 : 34 : 54 : 6) mixture with discharge currents of typically 500 nA and pressures of approximately 0·5 Torr.

Photons emitted from the discharge were observed by a linear collimator, 0·25 m monochromator and photomultiplier system, which could be traversed across the discharge in the y-direction at a given axial position z. This system measured the integrated photon count rate along a line of sight, the x-direction. The axial position of observation could be changed by moving the entire electrode assembly axially past the collimator. The linear collimator had an on-axis spatial resolution of 1·2 mm FWHM which corresponds to ≈2% of the internal radial dimension of the drift space.

The 337 nm band of the second positive system and the 391 nm band of the first negative system of molecular nitrogen were selected for study since they have excitation thresholds of 11·03 and 18·75 eV respectively. These thresholds are sufficiently well separated to expect that their relative intensities would be sensitive to small changes in the mean energy of the electrons. In order to obtain sufficient photon count rates in the 391 nm band at large axial positions and so yield accurate spatial distributions, it was necessary to use large E/N values. The integrated line of sight count rates for the two bands are shown in Fig. 3*a* for $z = 2 \cdot 5$ cm, using the $CO_2 : N_2 : He : CO$ mixture under conditions similar to those indicated in Fig. 1, i.e. $p_0 = 0 \cdot 373$ Torr and $E/N = 300$ Td. This value of z was chosen so that $\lambda_L z$ (and $\lambda_T z$) $\gg 1$, as required for the energy distribution function to be independent of the cathode boundary conditions.

The radial distribution of excited states can be obtained by Abel inversion of this integrated line of sight data. This was achieved by assuming that the radial distribution for any excited state could be described by the sum of truncated gaussian functions, i.e.

$$n_{ex}(r) = \sum_m b_m \left(\frac{a_m}{\pi}\right)^{\frac{1}{2}} \{\exp(-a_m r^2) - \exp(-a_m R^2\}, \qquad r \le R$$
$$= 0, \qquad r \ge R. \tag{5}$$

This is the Abel inversion of the line of sight integrated population

$$n_{ex}(y) = \sum_m b_m \left(\exp(-a_m y^2)\,\mathrm{erf}(c_m) - \frac{2c_m}{\pi}\exp(-a_m R^2)\right), \tag{6}$$

where $c_m = \{a_m(R^2 - y^2)\}^{1/2}$.

Using four terms in the summation, equation (6) was fitted to the experimental data using a least squares fitting procedure and the resuslts are shown as the solid curves in Fig. 3*a*. The fitting parameters a_m and b_m ($m = 1$ to 4) were

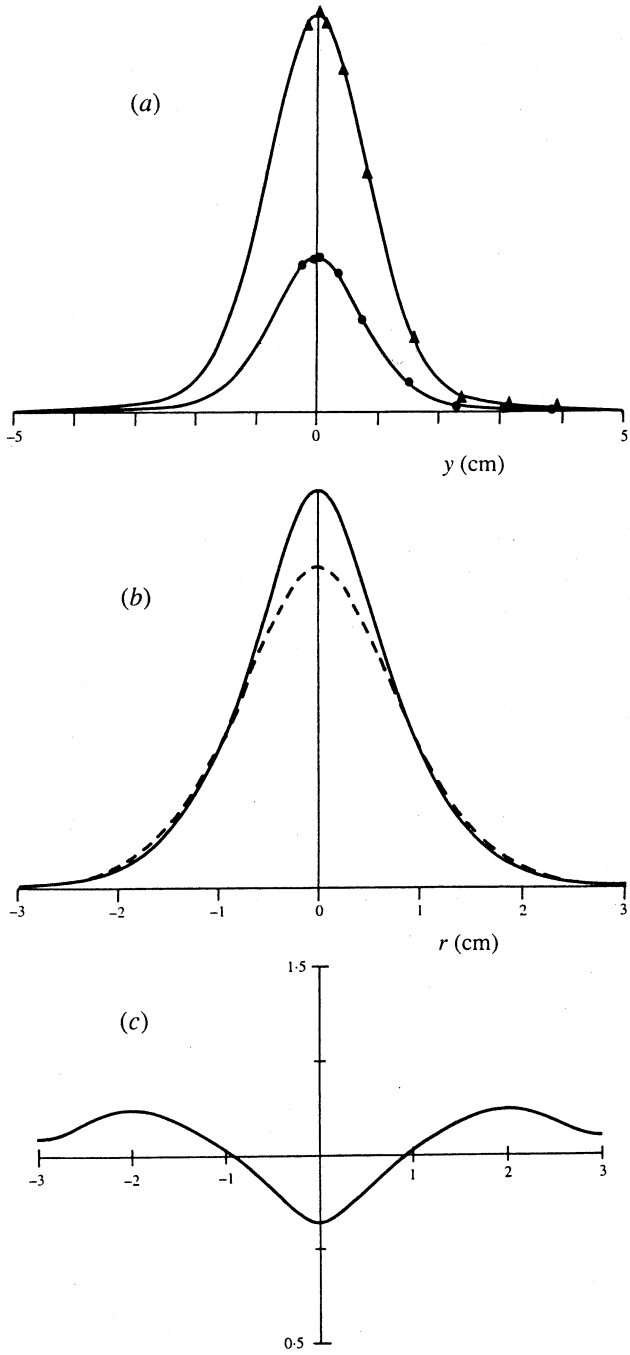

Fig. 3. (*a*) Comparison between the experimental line of sight data for the two excited states (the larger peak is the 337·1 nm data) and the least squares fit of equation (6) for $z = 2 \cdot 5$ cm. (*b*) Normalised Abel inversions $n_{ex}(r)$ given by equation (5) for 337·1 nm (solid curve) and 391·4 nm (dashed curve). (*c*) Radial variation in the excited state ratio $N(r,z)$ for $z = 2 \cdot 5$ cm.

then used in equation (5) to determine the radial dependence of the excited state populations, $n_{ex}(r)$. For a given axial position, the profile for the 391 nm band was normalised to the same radially integrated counts obtained for the 331 nm band. This normalisation of the line of sight data removes from consideration factors such as the wavelength dependence of the efficiency of the photon detection system and the lifetime of the excited states. It is a reasonable assumption that the excited molecules do not diffuse appreciably during the short lifetimes of these states, $\tau < 65$ ns. The results of the inversion given by equation (5) are shown in Fig. 3*b*. The ratio of the normalised excited state distributions $n_{ex}(r,z)$ for the two bands could then be determined and would be expected to be unity for all radial positions if there is no dependence of the electron energy distribution function on concentration gradients. However, the ratio $n_{ex}(337)/n_{ex}(391)$ is shown in Fig. 3*c* and indicates a significant radial variation.

As a test of the reliability of the results, the inversion procedure was repeated using two and three gaussians in equation (6) to describe the data. The excited state ratio rapidly converged to the four term solution shown in Fig. 3*c* which gives satisfactory results in the main body of the discharge.

4. Excited State Densities

A Monte Carlo simulation of electron swarms in hydrogen (Blevin *et al.* 1978) has shown that there is not a direct proportionality between electron concentration and the production of excited states. In a steady-state discharge $n_{ex}(r,z)$ is proportional to the excitation frequency $\nu_{ex_j}(r,z)$, so that from equation (4)

$$n_{ex_j}(r,z) = k_j\, n(r,z)\left\{\nu^0_{ex_j} - \left(\frac{1}{\lambda_L\, n(r,z)}\,\frac{\partial n(r,z)}{\partial z}\right)\nu^1_{ex_j}\right\}, \tag{7}$$

where k_j depends upon the lifetime of the state and efficiency of the detection system. Integrating over all radial positions and using the relationship $n(z) = \text{const.}\exp(\alpha_T z)$ (for regions not too close to the anode), we have

$$n_{ex_j}(z) = k_j\, n(z)\,\nu^0_{ex_j}\left(1 - \frac{\alpha_T}{\lambda_L}\,\frac{\nu^1_{ex_j}}{\nu^0_{ex_j}}\right)$$

If $j = 1$ and 2 refer to the $337\cdot1$ and $391\cdot4$ nm bands respectively, the normalisation procedure described in Section 3 is equivalent to equating $n_{ex_1}(z) = n_{ex_2}(z)$ and yields the condition

$$\frac{k_1\,\nu^0_{ex_1}}{k_2\,\nu^0_{ex_2}}\left\{1 - \frac{\alpha_T}{\lambda_L}\left(\frac{\nu^1_{ex_1}}{\nu^0_{ex_1}} - \frac{\nu^1_{ex_2}}{\nu^0_{ex_2}}\right)\right\} = 1,$$

where the gradient terms are assumed to be small.

Using this result and equation (7), again assuming that the concentration gradient terms are small, then the ratio of the normalised excited state populations can be given by

$$N(r,z) = \frac{n_{ex_1}(r,z)}{n_{ex_2}(r,z)} \approx 1 - \frac{1}{\lambda_L}\left(\frac{1}{n(r,z)}\,\frac{\partial n(r,z)}{\partial z} - \alpha_T\right)\left(\frac{\nu^1_{ex_1}}{\nu^0_{ex_1}} - \frac{\nu^1_{ex_2}}{\nu^0_{ex_2}}\right) \tag{8}$$

This equation represents both the first order ionisation correction and the local gradient correction to describe the non-uniform plasma. Since the 391·4 nm band has a higher threshold energy than the 337·1 nm band, it would be expected that its excitation would be more sensitive to changes in the mean energy and $\nu^1_{ex_1}/\nu^0_{ex_1} - \nu^1_{ex_2}/\nu^0_{ex_2}$ would be a negative quantity. Then we would have

$$N(r,z) - 1 \propto \frac{1}{\lambda_L n(r,z)} \frac{\partial n(r,z)}{\partial z} - \frac{\alpha_T}{\lambda_L}. \tag{9}$$

Comparing the experimental results of Fig. 3*c* with the theoretical values of $(1/\lambda_L n)\partial n/\partial z$ shown in Fig. 2, it is seen that the qualitative features of the experimental results are well described by the theory in the central regions of the discharge. However, there is a marked departure from the theoretical predictions in the outer regions of the discharge where the electron concentration is small relative to the central concentration. Although the extreme wings of the distribution are where the count rate approaches the background level, and hence less confidence can be placed in the Abel inversion procedure, this feature was observed at various axial positions $z = 0{\cdot}4, 0{\cdot}8$ and 2·5 cm), and with all gas mixtures used. An explanation of this behaviour is presented in the following section.

5. Discharge Characteristics at Larger Radii

The decrease in the experimental ratio $N(r,z)$ for larger values of r shown in Fig. 3*c* indicates that the axial concentration gradients in the outer regions of the discharge are not as large as the theory predicted from equation (1) (see Fig. 2). Moreover the observed count rate at large radii was greater than that expected from this equation. It is concluded that the additional electrons in this region of the discharge originate from a diffuse source of secondary electron production, a result of the high E/N. Secondaries produced from an ion avalanche returning to the cathode would result in a broad source with a distribution similar to that of the electron stream at the anode. Photon and metastable produced secondaries would be characterised by an even more diffuse source. Irrespective of the origin of the secondary electron emission, the spatial distribution of avalanches generated by secondary electrons is broader than that of the primary avalanche from the point source. In the outer regions of the discharge $n(r,z)$ is eventually dominated by the secondary electrons and approximates the distribution for a one-dimensional Townsend discharge. In this case $(1/n)\partial n/\partial z \approx \alpha_T$ and equation (8) shows that $N(r,z) \approx 1$.

To illustrate this more quantitatively we assume that (at the observation plane) the secondary electrons produce a distribution which is proportional to the first radial mode of the diffusion equation $J_0(\gamma_1 r/R)$, where γ_1 is the first root of $J_0(x)$ and R is the internal radius of the guard rings. This representation contains the feature of a broad source distribution and results in a particularly simple solution for the electron concentration $n(r,z)$ in the discharge volume. From the continuity equation the electron concentration can be shown to be (neglecting the anode boundary region)

$$n(r,z) = \text{const.}\left(\lambda_L z \exp(\lambda_L z)\frac{K_{3/2}(S_1)}{S_1^{3/2}} + AJ_0(\gamma_1 r/R)\exp(\beta z)\right), \tag{10}$$

where

$$\beta = \lambda_L \left\{ 1 - \left(1 + \frac{\gamma_1^2}{\lambda_L R \lambda_T R} - \frac{2\nu_i^0}{W\lambda_L} \right)^{\frac{1}{2}} \right\},$$

and A is constant and a measure of the total secondary electron production. This expression can be used to calculate $(1/\lambda_L n)\partial n/\partial z$ for various proportions of secondaries relative to the total electron number, as shown in Fig. 4.

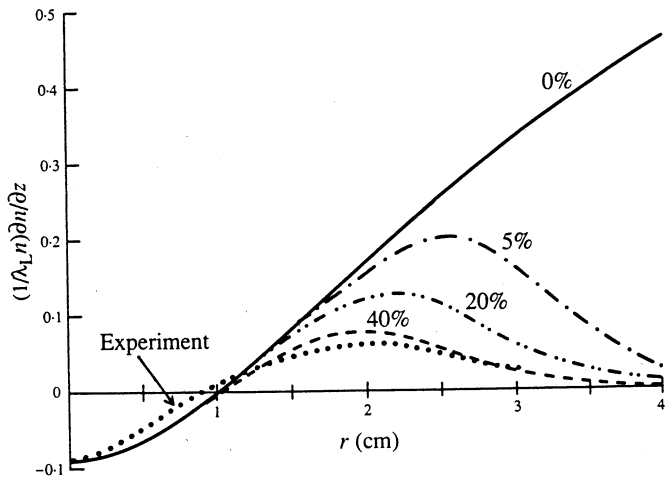

Fig. 4. Qualitative comparison between the experimental and theoretical ratio of excited states $N(r,z)$ for $z = 2{\cdot}5$ cm. The ratios are shown for 0%, 5%, 20% and 40% secondary electron contributions (as given by equations 9 and 10) and the experimental ratio data are normalised at $r = 0$.

While it requires approximately 40% secondary contribution to qualitatively describe the experimental results for larger radii, it must also be realised that the approximation used to describe the secondary source radial distribution may be inappropriate to account for all sources of secondary production. As previously mentioned the theory also makes no allowance for perturbations due to the cathode non-equilibrium region. This may explain the difference in structure of the experimental results at small radii (see Fig. 4). It should also be noted that under the present experimental conditions the resultant secondary electron density is small when compared with the localised primary electron density near the point source. As expected from the earlier discussion, it is clear that the secondary electron source plays an important part in an understanding of the experimental results at large radii, but has little influence on the structure of the results near the centre of the discharge provided that gas breakdown conditions are not approached.

6. Conclusions

The experimental results described here show that spatial variations in reaction rates occur in Townsend discharges as a consequence of the electron concentration gradients which always exist in a finite system with a localised electron source. These results are in general agreement with the theoretical model, although a truly quantitative analysis of the experiments will require further work. Obvious improvements to the experiment could be made by minimising secondary electron production by working with lower *pd* (gas pressure times electrode separation) values. Additionally, the nature of the secondary electron emission process could be studied by observing variations in photon emission at constant axial positions *z*, while *pd* is increased towards breakdown.

The spatial dependence of the excitation rates shown in Fig. 3*c* is significant and suggests analysis of experiments of this type should possibly be extended to include higher order terms in the gradient expansion of the electron energy distribution function. It is clear from the experiments described here that it is necessary to clarify procedures used to determine excitation rates in Townsend discharges and care must be taken in comparing these with theoretical predictions which may be based on the distribution function $g^0(\epsilon)$ alone. This could give rise to substantial errors at high *E/N* values, where α_T/λ_L is larger, or in electronegative gases where attachment produces large electron concentration gradients.

Earlier measurements utilising the photon flux technique (Fletcher and Blevin 1981) of secondary electron production by positive ion impact at the cathode have shown the importance of the atomic ion species in both N_2 and H_2 discharges. Since dissociative ionisation has a relatively large threshold energy, then the present work indicates that the ionisation frequency for this process will have a strong spatial dependence. This should be taken into account in consideration of the radial variation of the secondary electron production at the cathode. Electron transport and ionisation coefficients which are independent of radial gradient influences can be simply obtained from photon flux experiments by considering the radially integrated emission (Wedding *et al.* 1985).

We conclude that experiments of the type discussed here are capable of a more comprehensive investigation of the internal characteristics of electron swarms than has been attempted previously. The spatial and temporal resolution and the dynamic range of the detection system are such as to encourage the development of experiments which will yield more quantitative information than can be obtained from the preliminary results described in this paper.

Acknowledgments

The authors are indebted to Prof. H. A. Blevin for his continual interest and contributions to this work and also wish to thank Drs A. V. Phelps and J. Fletcher and Mr A. M. Garvie for constructive discussions. This work has been supported in part by the Australian Research Grants Scheme. One of us (L.J.K.) was the recipient of a Commonwealth Research Scholarship during the course of this work.

References

Blevin, H. A. (1985). Seventeenth Int. Conf. on Phenomena in Ionised Gases, Budapest 1985 (Eds J. S. Bakos and Z. S. Uzsa Sörlei), p. 308.
Blevin, H. A., and Fletcher, J. (1984). *Aust. J. Phys.* **37**, 593.
Blevin, H. A., Fletcher, J., and Hunter, S. R. (1978). *J. Phys.* D **11**, 1653.
Fletcher, J., and Blevin, H. A. (1981). *J. Phys.* D **14**, 27.
Huxley, L. G. H. (1972). *Aust. J. Phys.* **25**, 43; 523.
Kumar, K., Skullerud, H. R., and Robson, R. E. (1980). *Aust. J. Phys.* **33**, 343.
Parker, J. H., and Lowke, J. J. (1969). *Phys. Rev.* **181**, 290.
Robson, R. E. (1981). *Aust. J. Phys.* **34**, 223.
Skullerud, H. R. (1969). *J. Phys.* B **2**, 696.
Tagashira, H., Sakai, Y., and Sakamoto, S. (1977). *J. Phys.* D **10**, 1051.
Thomas, W. R. L. (1969). *J. Phys.* B **2**, 551.
Wedding, A. B. (1985). *J. Phys.* D **18**, 2351.
Wedding, A. B., Blevin, H. A., and Fletcher, J. (1985). *J. Phys.* D **18**, 2361.

Manuscript received 20 April, accepted 28 July 1988